

# A FUEL-PAYLOAD RATIO BASED FLIGHT-SEGMENTATION BENCHMARK

Kim Kaivanto<sup>§\*</sup> and Peng Zhang<sup>‡</sup>

<sup>§</sup>Lancaster University, Lancaster LA1 4YX, UK

<sup>‡</sup>Guizhou Minzu University, Guiyang City, PRC 550025

*this version:* May 8, 2018

## Abstract

Airlines and their customers have an interest in determining fuel- and emissions-minimizing flight segmentation. Starting from Küchemann's Weight Model and the Breguet Range Equation for cruise-fuel consumption, we build an idealized model of optimal flight segmentation for maximizing fuel efficiency and minimizing emissions under the assumption that each leg is operated with an aircraft of segment-length-matching design range. When a multi-leg ( $\geq 2$ ) itinerary is most efficient, legs are ideally of equal length. Instrumental to the parsimony of this flight-segmentation benchmark is a new efficiency metric: Fuel-Payload Ratio (FPR). The FPR approach has a one-to-one correspondence with the standard microeconomic cost-curves framework, which avails the standard tools of microeconomic analysis for cost-efficient design-range determination and optimal flight segmentation. This makes it possible to make direct comparisons between (i) technically efficient design-range and flight-segmentation solutions and (ii) their economically efficient counterparts. Even modest fixed-cost components cause the latter to diverge non-trivially from the former.

*Keywords:* scheduled passenger air transport, flight segmentation, fuel efficiency, greenhouse gas emissions, microeconomics

*JEL classification:* Q54, D62, D03, L93

---

\*Corresponding author: tel +44(0)1524594030; fax +44(0)1524594244; e-mail k.kaivanto@lancaster.ac.uk

# 1 Introduction

Air transportation is caught between two converging fronts. The first is increasing demand for air transportation, driven by income growth – notably, at a rate faster than income growth itself – during an era of consistently increasing world Gross Domestic Product (GDP).<sup>1</sup> The second is accelerating anthropogenic climate change, and the consequent need to reduce greenhouse gas (GHG) emissions drastically in order to avoid global-ecosystem-altering climate change. Technological innovation and far-reaching policy changes will be required in the medium term in order to achieve the targets agreed to in the United Nations Framework Convention on Climate Change (UNFCCC COP21).

But in the short run, the GHG footprint of air transportation can be reduced by optimizing aircraft design-and-deployment decisions within the envelope of current technological possibility. This builds upon and makes the most of ongoing technological innovation to improve the efficiency of propulsion technology, improve wing and airframe strength-to-weight ratio by the introduction composite technology, and improve aerodynamic efficiency by e.g. the introduction of winglet technology (Cansino and Román, 2017).

Although several methods exist for calculating the GHG emissions of scheduled air transport, the dominant component common to all methods is *mission fuel* (see e.g. Kaivanto and Zhang, 2017). Nevertheless mission fuel is not the only determinant of GHG emissions. Non-fuel-based measures – such as lowering the cruise altitude<sup>2</sup> and rerouting aircraft trajectories in real time to mitigate persistent contrail formation – are potentially important complementary components of emissions-reduction policy packages (Dallara and Kroo, 2011; Campbell et al., 2013). In the present paper however, the focus is on fuel and the possibilities for economizing on fuel burn through optimal flight segmentation.

Whereas route-structure variables are among the many that airlines and air-transport authorities typically optimize jointly (e.g. Dumas et al., 2009; Li et al., 2010; Pita et al., 2014; Dalmau and Prats, 2015), here we tackle the flight-segmentation aspect of route structure in

---

<sup>1</sup>In the post-1970s era, GDP has consistently grown, with the exception of one year in which the world economy absorbed the fallout from the financial crisis (2009). The empirical income elasticity of demand for air transportation services is widely documented to be greater than 1: for every 1% increase in income (i.e. GDP), demand for air transport increases by *more* than 1% (IATA, 2008; Chi and Baek, 2012; Gallet and Doucouliagos, 2014).

<sup>2</sup>(i) to reduce the impacts of NO<sub>x</sub> emissions and (ii) to reduce the likelihood of persistent contrail formation

isolation. By doing so, we abstract from the numerous variables and considerations for which fuel burn and GHG emissions are traded off in joint optimization exercises. In this sense, we investigate a pure – and therefore idealized – fuel- and emissions-focused flight-segmentation benchmark.<sup>3</sup>

This problem definition is not without precursors in the literature. Yutko and Hansman (2011) report<sup>4</sup> the frequencies of operations (legs flown) by all US carriers at different fractions of design range ( $R_1$ ), separately for narrow-body aircraft, wide-body aircraft, and regional jets.<sup>5</sup> The mean of narrow-body aircraft operations was at 41% of  $R_1$ ; the mean of wide-body aircraft operations was at 61% of  $R_1$ ; and the mean of regional-jet aircraft operations was at 39% of  $R_1$ . Virtually all passenger air-transport movements are therefore sacrificing fuel and emissions efficiency by being operated with aircraft of much greater design range. Zeinali and Rutherford (2010) also document this “inferior environmental performance during actual operation” and suggest that it may be the result of a ‘one-size-fits-all’ approach in which aircraft are sized to meet extreme missions – presumably to offer the greatest possible scope for flexible deployment – rather than to meet representative payload-range missions. Thus, modern jet aircraft are oversized and consequently less efficient in operation than current technology is capable of delivering. Accordingly Zeinali and Rutherford (2010) identify “aircraft rightsizing” as a means of realizing efficiency improvements and emissions reductions – which they identify as a key challenge for the International Civil Aviation Organization (ICAO).

In turn Perez and Jansen (2014) advocate coupled design optimization, in which the aircraft’s design configuration is optimized specifically for taking advantage of Intermediate Stop Operations (ISOs). The question of how ISO routes should be designed to maximize fuel and GHG efficiency is also broached by Green (2002), but his recommendations are couched in preliminary and suggestive language.<sup>6</sup> Poll (2011) revisits this question, and finds that significant fuel- and GHG-related savings are only available for distances greater than 5,500 km. Martinez-Val et al.

---

<sup>3</sup>Even though there may currently be practical impediments to full implementation of the present idealized flight-segmentation method, shifts toward this benchmark yield efficiency improvements. This is similar in spirit to Dalmau and Prats’ (2015) proposal, also published in *TRD*, for achieving fuel and time savings by flying continuous-cruise climbs, rather than the constant-cruise-altitude flight levels currently operated under Air Traffic Control (ATC) direction.

<sup>4</sup>in their analysis of 2006 Bureau of Transportation Statistics (BTS) Form 41 T-100 data

<sup>5</sup>in their Figures 16, 17 and 18, respectively.

<sup>6</sup>For instance: “...the full report ... leads to the suggestion that the most environmentally friendly solution might be to break long journeys into sectors not exceeding 7,500 km...” (p 61 Green, 2002)

(2013) and Langhans et al. (2013) also begin with this question, but find that there is a tension between the engineering objectives of achieving fuel savings and reducing environmental impact, on the one hand, and economic cost efficiency, on the other hand. Our investigation aims to synthesize and deepen the aforementioned results parsimoniously.

This paper’s novel contributions range across three dimensions.

*First*, the Fuel-Payload Ratio (FPR) efficiency measure – although derived from the same set of equations Green (2002, 2006) employs – has a direct interpretation in the standard microeconomic framework as the lower envelope of Total Variable Input (TVI) curves, which avails all of the standard microeconomic analysis tools. Using this microeconomic framework, we illustrate how Fixed Costs affect Average-Total-Cost-minimizing design range, thereby contributing to our understanding of the empirical disparity between the design ranges of aircraft purchases (and stock thereby created) based on economic drivers and the design ranges of aircraft purchases (and associated stock created) if they were guided purely by technical (fuel, GHG) efficiency.

*Second*, the present study of flight segmentation aims to sharpen Green’s (2002) somewhat vague suggestions concerning efficiency-maximizing stage length. Hence the present study is distinct from, but responds to, complements, and sharpens Green (2002). The advantage of the FPR-based approach is that its mathematical form provides straightforward answers to these types of questions.

*Third*, the sensitivity analysis reported in this study investigates the effects of perturbations in (i) the ‘lost-fuel’ fraction  $\lambda$  of take-off weight that is consumed during takeoff, climb-to-cruise altitude and acceleration-to-cruise speed, and (ii) the range-performance parameter  $X$ , which is a composite of propulsive efficiency and aerodynamic efficiency. In contrast, Green’s (2002) sensitivity analysis studies the effects of perturbations in structural constants of proportionality pertaining to maximum take-off weight and payload. Hence the present study is distinct from, but complements Green (2002).

In Section 2 we investigate the impact of design range on commercial air transport fuel efficiency by developing a model drawing on Küchemann’s (1978) Weight Model and the Breguet Range Equation for cruise fuel consumption. These two equation families complement each other. Küchemann’s (1978) Weight Model is a standard if not classic<sup>7</sup> decomposition of aircraft

---

<sup>7</sup>Dietrich Küchemann is thought by some to be the finest aerodynamicist of his generation. His posthumously published (1978) *The Aerodynamic Design of Aircraft* is widely regarded as a classic text in aerodynamics.

take-off weight into components that roughly correspond to airframe empty weight, payload, engines, and mission fuel. The Breguet Range Equation in turn allows cruise range to be expressed as a function of (i) aircraft initial weight at take-off, (ii) aircraft ‘final weight’ upon landing, after mission fuel has been consumed, and (iii) range-performance parameters capturing the calorific energy content of the fuel, the propulsive efficiency of the engine, and the aircraft design’s lift-to-drag ratio. Using these equations Green (2002) derived the Payload Fuel Efficiency (PFE) metric, defined as the product of range and the ratio of the weight of payload to mission fuel. We build on this in Section 3 to introduce a new efficiency metric, the Fuel-Payload Ratio (FPR), which captures the technical relationship between mission fuel burn and payload transported to design range. With the aid of this FPR metric, identification of optimal design range (Section 3.2), as well as optimal thresholds for 1-, 2-, and 3-segment flights (Section 3.3), is straightforward. Furthermore,  $1/\text{FPR}$  may be understood as a short-run production function in a standard microeconomic sense, from which it follows that the standard short-run curves – marginal and average product, variable cost and total cost, marginal cost, average variable cost and average total cost – may also be derived straightforwardly. This makes it possible to undertake economic optimization of the design-range decision parsimoniously, without abstracting from any of the the engineering information contained in Green’s (2002) PFE metric. We conclude with a sensitivity analysis (Section 4) that complements rather than replicates the sensitivity analysis undertaken in Green (2002).

## 2 Flight-range design for fuel efficiency

In the past two decades the literature on optimal aircraft design for environmental impact reduction has become an important stream within air transport research (Lee et al., 2001; Green, 2009; Dallara, 2011; Dallara and Kroo, 2011). Specifically, the relationship between design range and fuel efficiency has drawn particular attention (Green, 2002, 2006). However, most studies in the literature opt for numerical illustration of theoretical predictions, and therefore an analytical treatment of this topic is often absent. In this section we present a model composed of well-known results in this literature, and we apply this analytical model to the problem of fuel- and emissions-efficiency.

## 2.1 Nomenclature

$c_1$	structural constant of proportionality related to maximum take-off weight
$c_2$	structural constant of proportionality related to payload
$H$	calorific value of fuel (energy per unit mass)
$OEW$	operating empty weight
$L/D$	lift-to-drag ratio at cruise
PFE	payload fuel efficiency
FPR	fuel-payload ratio
$R$	design range
$W_E$	weight of engine
$W_{MF}$	weight of mission fuel
$W_P$	weight of payload
$W_{TO}$	aircraft weight at takeoff
$W_{initial}$	aircraft weight at the beginning of cruise
$W_{final}$	aircraft weight at the end of cruise
$X$	aircraft range parameter
$\lambda$	the fraction of aircraft weight at takeoff as lost fuel
$\eta$	overall propulsive efficiency

## 2.2 Theory

Küchemann (1978) proposes a basic decomposition of aircraft weight at take-off, which consists of four components.

$$W_{TO} = c_1 W_{TO} + c_2 W_P + W_E + W_{MF} \quad (1)$$

The first term captures necessary mass elements of the aircraft. The second term represents payload and the fittings/furnishings that vary in proportion to payload. The third term is the fixed weight of engines. The last term is the weight of mission fuel.

Green (2002) simplifies this model further by assuming that engine weight is also proportional to the total weight at takeoff and can be incorporated into  $c_1$ , resulting in the following

$$W_{TO} = c_1 W_{TO} + c_2 W_P + W_{MF} \quad (2)$$

As in Green (2002), we introduce the Breguet Range Equation as

$$R = X \ln \left( \frac{W_{\text{initial}}}{W_{\text{final}}} \right) \quad (3)$$

where  $R$  represents the design range and  $X$  represents a range-performance parameter defined as

$$X = H\eta \frac{L}{D} \quad (4)$$

where  $H$  is the calorific value of the fuel,  $\eta$  is the overall propulsion efficiency of the engine and  $\frac{L}{D}$  is the lift-to-drag ratio of the aircraft at cruising speed.

Assume that ‘lost fuel’ – defined as fuel consumed during takeoff, climb-to-cruise altitude and acceleration-to-cruise speed (Torenbeek, 1997) – weighs a fraction  $\lambda$  of aircraft weight at takeoff ( $\lambda W_{\text{TO}}$ ). Then we have

$$W_{\text{initial}} = (1 - \lambda)W_{\text{TO}} \quad (5)$$

$$W_{\text{final}} = W_{\text{initial}} - (W_{\text{MF}} - \lambda W_{\text{TO}}) \quad (6)$$

where  $W_{\text{MF}}$  represents the total mission fuel weight. In Green (2002),  $\lambda$  is assumed to be 2.2%, while in the present study we take a more general approach and investigate the impact of the parameter value. Substituting equations (5) and (6) into the Breguet range equation yields

$$W_{\text{MF}} = W_{\text{TO}} \left( 1 - \frac{1 - \lambda}{\exp \left( \frac{R}{X} \right)} \right) \quad (7)$$

By combining this with equation (2) and rearranging, we have the mission fuel weight as a function of range and payload weight.

$$W_{\text{MF}} = \left( \frac{1}{1 - \lambda} \exp \left( \frac{R}{X} \right) - 1 \right) \frac{c_2}{1 - \frac{1}{1 - \lambda} \exp \left( \frac{R}{X} \right) c_1} W_{\text{P}} \quad (8)$$

The Greener by Design Technology Sub Group (2002) characterizes fuel efficiency with ‘Payload Fuel Efficiency’ (PFE) defined as the ratio of the product of range and payload to mission fuel:

$$\text{PFE} = \frac{R \cdot W_{\text{P}}}{W_{\text{MF}}} \quad (9)$$

Combining equations (8) and (9) yields

$$\text{PFE} = \frac{R(1 - \lambda - \exp\left(\frac{R}{X}\right) c_1)}{c_2(\exp\left(\frac{R}{X}\right) - 1 + \lambda)} \quad (10)$$

The efficiency maximization problem can be expressed as

$$\max_R \text{PFE} \quad \text{s.t.} \quad R \geq 0 .$$

The derivative of PFE with respect to design range ( $R$ ) is a nonlinear function, and therefore optimal  $R$  cannot be solved for easily in closed form. We follow Green (2002) in employing a numerical approach to illustrating the properties of this maximization problem, and conduct a sensitivity analysis in Section 4.

### 2.3 Numerical illustration

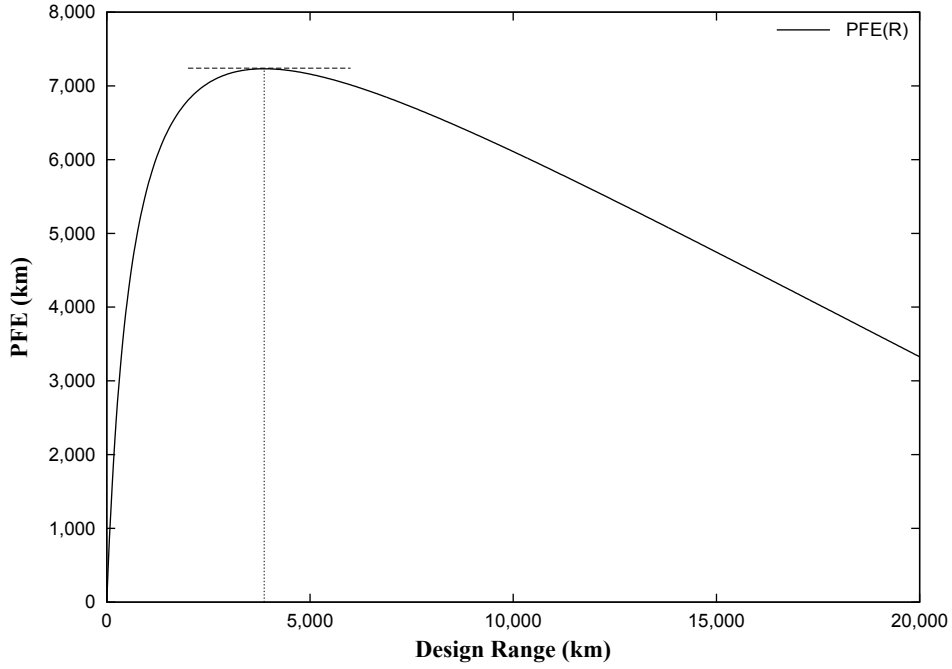
In order to illustrate how PFE varies with design range, parameter values need to be determined for  $X$ ,  $\lambda$ ,  $c_1$  and  $c_2$ . Using Fielding's (1999) data, Green (2002, 2006) estimates  $c_2$  to be 2.0. Green (2006) revisits the estimation of  $c_1$  in light of Nangia (2006), and using Fielding's (1999) data Green (2006) estimates  $c_1$  to be 0.345.<sup>8</sup> We also follow Green (2002, 2006) in employing the aircraft range parameter  $X = 30,580\text{km}$  and the lost-fuel fraction  $\lambda = 2.2\%$ . Substituting these parameter values into equation (10) and plotting PFE against range  $R$ , we obtain Figure 1.

Figure 1 verifies Green's (2006) finding that efficiency measured by PFE is a concave function of design range and reaches maximum when design range is in the region of 3,872km for a typical wide-body swept-wing kerosene-fueled aircraft. When design range is shorter than 3,872km, a large fraction of mission fuel is consumed in the take-off and climb stage, leading to low efficiency. When design range exceeds 3,872km, a large mass of mission fuel will be carried for a long distance before combustion, leading to decreasing efficiency as design range is pushed beyond 3,872km.

---

<sup>8</sup>These values for  $c_1$  and  $c_2$  are obtained by fitting  $OEW = (c_1 - 0.045)W_{\text{TO}} + (c_2 - 1)W_{\text{P}}$  to Fielding's (1999) Table A4.5 (page 188) data on twelve modern wide-body, swept-wing, kerosene-fueled passenger aircraft, where the parameter 0.045 reflects Nangia's (2006) estimate that reserve fuel comprises 4.5% of total weight at takeoff (Green, 2006).

Figure 1: Payload fuel efficiency against design range: Wide-body swept-wing kerosene-fueled aircraft.



### 3 Optimal flight segmentation – a new approach

#### 3.1 Fuel-Payload Ratio

We develop a new approach to the finding in Section 2 that yields new insight into the theory, particularly with regard to economizing on GHG emissions achieved through optimal flight segmentation. Instead of focusing on Payload Fuel Efficiency (PFE), we propose a new metric, the *Fuel-Payload Ratio* (FPR), defined as the ratio of mission fuel weight to payload weight. Following the above-developed model based on Küchemann’s Weight Model and the Breguet Range Equation, FPR can be written as

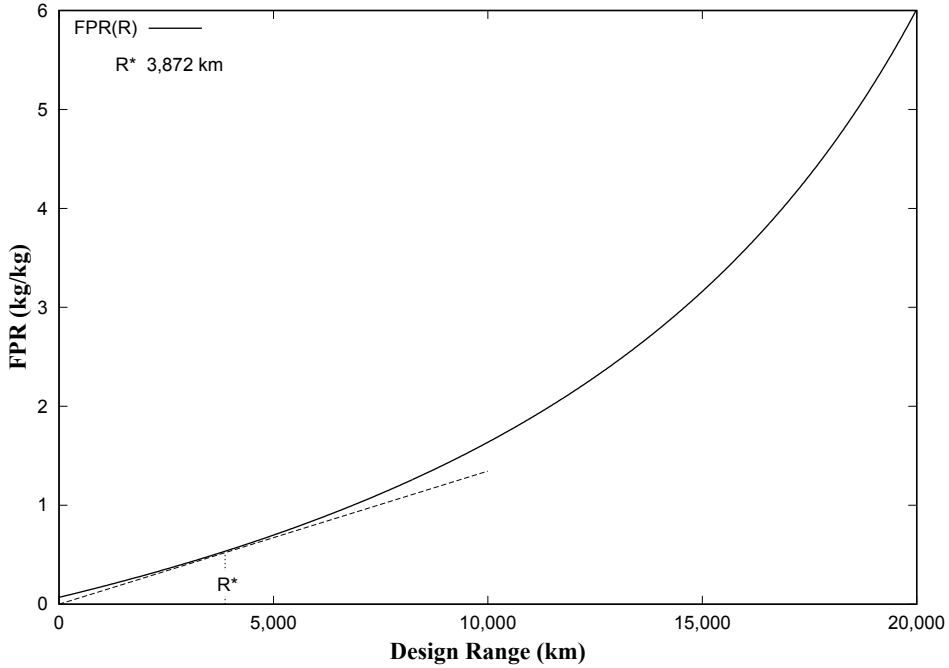
$$\text{FPR}_R = \left( \frac{W_{\text{MF}}}{W_{\text{P}}} \right)_R = \frac{\exp\left(\frac{R}{X}\right) - 1 + \lambda}{1 - \lambda - \exp\left(\frac{R}{X}\right) c_1} \cdot c_2 \quad (11)$$

This ratio measures the mission fuel required to deliver a one-unit payload to a specified range, using an ideal aircraft with matching design range. We will show that, compared to efficiency measured by the PFE factor introduced in Section 2, a re-description of the same model using this ratio brings new insight regarding fuel efficiency and GHG-emissions reduction, in particular where flight segmentation is concerned.

### 3.2 Numerical illustration

In this numerical example, we continue to employ the parameter values introduced above in Section 2.3.<sup>9</sup> Substituting these parameter values into equation (11) and plotting FPR against range  $R$ , we obtain Figure 2.

Figure 2: Fuel-Payload Ratio against design range: Wide-body swept-wing kerosene-fueled aircraft.



Several observations may be made regarding FPR.

**Finding 3.1 (Mission fuel increases with  $R$ , at an accelerating rate).** For a typical swept-wing kerosene-fueled aircraft, FPR is a convex function of design range. The total weight of mission fuel required to deliver a one-unit payload to the design range is increasing in design range at an accelerating rate. Furthermore, this increasing rate ( $f'' > 0$ ) is itself increasing ( $f''' > 0$ ). This is due to the fact that as design range increases, more fuel will be carried for a longer distance before combustion, creating a self-reinforcing feedback loop in the mission fuel required.

**Finding 3.2 (min FPR/km design range =  $R^*$ ).** Figure 2 also contains information regarding Payload Fuel Efficiency from Figure 1. If we draw a line segment from the origin to any

<sup>9</sup> $c_1 = 0.345$ ,  $c_2 = 2.0$ ,  $\lambda = 2.2\%$ ,  $X = 30,580$  km

point along the FPR curve, the slope of this line segment is equal to the inverse of the Payload Fuel Efficiency, i.e.  $1/\text{PFE}$ . The FPR curve's vertical intercept is at  $(0, 0.070)$ .<sup>10</sup> As the line segment's end point on the FPR curve moves to the right from the vertical intercept, the slope first decreases, and then eventually increases. The lowest-slope line segment from the origin is tangent to the curve at the abscissa coordinate associated with a design range of 3,872km (rounded to the nearest km). At this design range

$$\frac{\text{FPR}}{R} = \frac{d\text{FPR}}{dR} \quad (12)$$

and

$$\arg \min \frac{\text{FPR}}{R} = \arg \min \frac{d\text{FPR}}{dR} = R^* \quad (13)$$

This is the design range at which minimum FPR/km is achieved.

**Finding 3.3 (FPR-based mission fuel is validated by ICAO data).** The FPR curve in Figure 2 fits empirical data well. Table 1 contains ICAO data on flight range, average mission-fuel consumption and average number of seats (columns 3–5).<sup>11</sup> Using these data, FPR values are calculated from Figure 2 and total mission fuel is calculated (rounded to the nearest integer) assuming a 150kg payload for each average seat. The departure and destination airports are chosen so that the data contain short-, medium-, long- and ultra-long-haul flights. We can see that the calculated mission fuel consumption (column 7) fits ICAO average fuel data (column 4) quite well, especially for medium and long range flights. This suggests that the FPR method in Figure 2 provides a reliable method for estimating mission fuel consumption, especially for medium- and long-haul flights.

**Finding 3.4 (Standard microeconomic interpretation).** In a microeconomic context the FPR curve in Figure 2 corresponds to the lower envelope of Total Variable Input (TVI) curves, where each  $\text{TVI}_{R'}$  curve is obtained as the locus of FPR when flying an aircraft optimized for

<sup>10</sup>The reason for positive mission fuel at zero range comes as a result of the simplified assumption that fuel for take-off, climb and manoeuvre stand as 2.2% of total weight of the aircraft at take-off, even when range decreases to zero. Zero and very small ranges are included mainly as part of a complete mathematical description and graphic demonstration, but it is understood that they lack meaningful interpretation in practice.

<sup>11</sup>ICAO (2012) documents the methodology by which the average fuel (kg) data have been compiled. The approach employed draws primarily from the EMEP/CORINAIR Emission Inventory Guidebook, following IPCC guidance.

Table 1: Average fuel burn ICAO vs. FPR-based mission-fuel calculation

Origin	Destination	Range (km)	Average fuel (kg)	Seats	FPR	Mission fuel (kg)
MAN	LGW	283	1,898	154	0.099	2,296
MAN	EDI	298	822	61	0.101	924
MAN	CDG	586	2,723	141	0.132	2,792
MAN	DXB	5,649	44,827	363	0.799	43,500
MAN	JFK	5,359	28,329	251	0.753	28,363
LHR	PEK	8,149	75,726	439	1.241	81,709
LHR	SIN	10,869	103,535	428	1.848	118,629

design range  $R'$  on legs of length  $[0, 20,000]$ .<sup>12</sup> Transposing the axes yields the

$$R = f(\text{FPR}) \quad (14)$$

curve, which has the microeconomic interpretation of the upper envelope of short-run ‘design-range’ production functions: the horizontal axis indicates the variable input (kg of mission fuel per kg of payload) and the vertical axis indicates the design range attained. Implicit in  $f(\cdot)$  is the current level of technology that embodies what could be stated explicitly as fixed capital  $K$ .

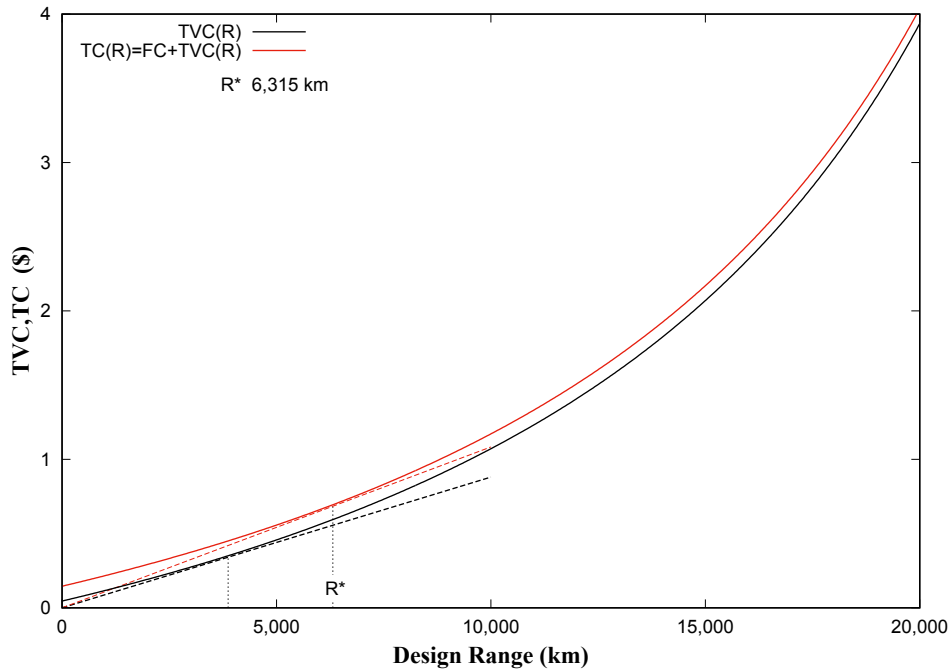
Placing FPR within a microeconomic framework leads to insights that are typically not available within a purely technical engineering analysis. For instance,  $\text{FPR}_R = \left(\frac{W_{MF}}{W_P}\right)$  may be re-expressed in monetary-unit terms by multiplying equation (11) by the price of kerosene (\$/kg) – i.e. the vertical axis of Figure 2 may be re-indexed by multiplying by the price of kerosene, which at the time of writing is 654.8 \$/mt or 0.6548 \$/kg (see Figure 3).<sup>13</sup> On this cost scale, the FPR becomes the lower envelope of Total Variable Cost (TVC) curves. This opens up the possibility of investigating the effect of changes in Fixed Costs (FC) on cost-efficient choice of design range – regardless of whether those Fixed Costs arise from engineering, regulatory (e.g. environmental regulations), safety and service, or other business-environment considerations. Figure 3 illustrates how a 10¢ increase in Fixed Cost<sup>14</sup> increases Average-Total-Cost-minimizing design range by over 2,400 km.

<sup>12</sup>Every range- $R'$ -optimized design has  $\text{FPR}_{(R')}$  values that lie on or above the FRP curve pictured in Figure 2.

<sup>13</sup>Jet fuel price obtained from The International Air Transport Association (IATA) Jet Fuel Price Monitor on 30 March 2018. <http://www.iata.org/publications/economics/fuel-monitor/Pages/index.aspx>

<sup>14</sup>per kg of payload

Figure 3: Total Variable Cost (TVC) and Total Cost (TC) envelopes against design range, where the Fixed Cost (FC) component of TC is 10¢ per payload kg.



This microeconomic analysis of the effect of Fixed Costs carries two types of implications. First, it goes some way to explaining why the stock of aircraft operated on short- and medium-length segments are ‘oversized’ in terms of design range: economic considerations rather than purely technical fuel- and GHG-efficiency considerations weigh heavily in the aircraft purchase decision. Second, it shows the unintended consequences of introducing regulations – whether motivated by environmental-protection concerns or not – that increase payload Fixed Cost.

Finally and perhaps most importantly, FPR brings new insight to fuel- and emissions-efficiency by providing guidance on optimal flight segmentation. We develop this in the next section.

### 3.3 Optimal route-segmentation benchmark

Compared to expressing efficiency through Payload Fuel Efficiency, the new representation in Figure 2 emphasizes mission fuel and GHG emissions directly. This advantage becomes particularly useful (i) when facing a choice between different route options for an origin-destination pair, (ii) at the airline set-up stage, or (iii) at the flight-choice stage for a commercial aviation consumer.

Consider efficiency as represented by PFE in Figure 1. While the PFE curve perfectly captures the changing fuel efficiency as a single aircraft is designed for a longer range, it is unclear how to compare the efficiency levels of multiple aircraft with different design ranges, when aircraft can be grouped to serve a route containing multiple segments. For example, for an origin-destination pair 10,000 Great-Circle km apart, would it be more fuel efficient and hence less environmentally harmful to choose a direct flight using an aircraft with a design range of 10,000km, or to divide the itinerary into segments? If the latter is more efficient, how many segments and how should the decision maker choose the segmentation optimally?

Answers to these questions are not straightforward from the PFE-based analysis.

The Fuel-Payload Ratio curve, on the other hand, provides straightforward answers to these questions.

Since FPR represents the ideal mission-fuel consumption to deliver a one-unit payload to a specified range, when the same unit payload is delivered through segments, the sum of segment-specific FPR ratios represents the total mission fuel for the whole itinerary, assuming that the ideal aircraft (with appropriate design range) is used on each segment. As the FPR curve is convex in design range, this offers unambiguous guidance for minimizing the sum.

We consider three cases: a direct itinerary, an itinerary with two segments, and an itinerary with three segments. These three cases will suffice for most origin-destination pairs, with the exception of ultra-long haul itineraries such as London to Sydney, where no direct-flight service is currently available from any airline. For simplicity assume that a transfer airport is always available at any point on the Great-Circle line connecting the origin and destination. Given the convexity of the FPR curve shown in Figure 2, it is straightforward to prove mathematically that for an itinerary with two segments, the optimal transfer airport is at the midpoint; for an itinerary with three segments, the optimal refueling airports divide the Great Circle line into equal thirds (see Appendix A).

The cutoff threshold between the one-segment-is-optimal interval and the two-segments-are-optimal interval is given by the solution to  $FPR_1 = FPR_2$ , that is the design range  $R$  that solves

$$c_2 \left( \frac{\exp\left(\frac{R}{X}\right) - 1 + \lambda}{1 - \lambda - \exp\left(\frac{R}{X}\right) c_1} \right) = 2c_2 \left( \frac{\exp\left(\frac{R/2}{X}\right) - 1 + \lambda}{1 - \lambda - \exp\left(\frac{R/2}{X}\right) c_1} \right). \quad (15)$$

Similarly, the cutoff threshold between optimality of two and three segments is given by the solution to  $FPR_2 = FPR_3$ , which is the design range  $R$  that solves

$$2c_2 \left( \frac{\exp\left(\frac{R/2}{X}\right) - 1 + \lambda}{1 - \lambda - \exp\left(\frac{R/2}{X}\right) c_1} \right) = 3c_2 \left( \frac{\exp\left(\frac{R/3}{X}\right) - 1 + \lambda}{1 - \lambda - \exp\left(\frac{R/3}{X}\right) c_1} \right). \quad (16)$$

We illustrate these cutoff thresholds graphically.

Using the same numerical estimates as in previous sections<sup>15</sup> we plot (in Figure 4) the FPR against design range for a direct flight, an itinerary segmented into two equal halves, and an itinerary segmented into three equal thirds. Recall that Figures 1 and 2 both suggest that the highest efficiency for a single-hop flight (a single takeoff-landing pair) is achieved at a design range of 3,872km. For distances shorter than 5,433km, dividing the itinerary would result in segments much shorter than the optimal 3,872km and thus a lower efficiency for the itinerary overall. Therefore the direct flight remains the most fuel- and hence GHG-efficient. For distances between 5,433km and 9,462km, an itinerary segmented into two equal halves is most efficient, as the fuel burn of a direct flight is considerably higher due to the inefficiently high fuel-load burden it requires. For distances above 9,462km, an itinerary segmented into three equal thirds becomes most efficient.

Exploiting the TVI interpretation of the FPR curve, we can re-examine the flight-segmentation problem from the standpoint of minimizing Total Cost (TC). Using the same price for jet fuel as was used above in Figure 3 (0.6548 \$/kg) and maintaining the assumption that Fixed Cost (FC) per payload kg per leg is 10 ¢, we plot (in Figure 5) the TC against design range for a direct flight, an itinerary segmented into two equal halves, and an itinerary segmented into three equal thirds. Notice that there are large differences between the technically efficient flight-segmentation thresholds (5433km and 9462km) and the economically efficient flight-segmentation thresholds (8800km and 15394km) – even when FC is limited to a very modest 10 ¢ per payload kg per leg.

---

<sup>15</sup>  $c_1 = 0.345$ ,  $c_2 = 2.0$ ,  $\lambda = 2.2\%$ ,  $X = 30,580$  km

Figure 4: Fuel-Payload Ratio against design range: direct flight, two-segment itinerary, and three-segment itinerary.

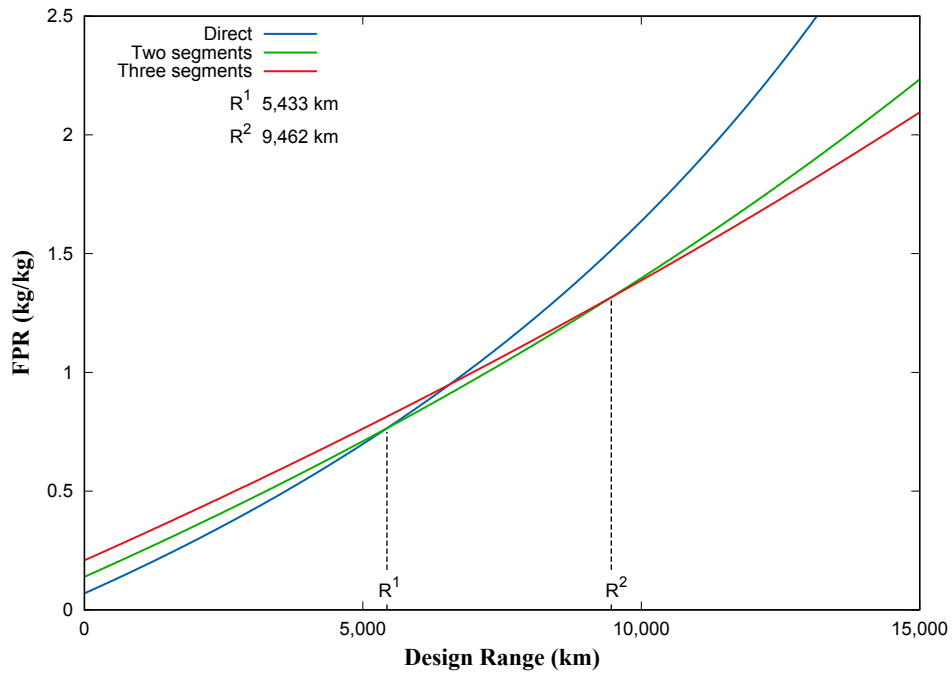
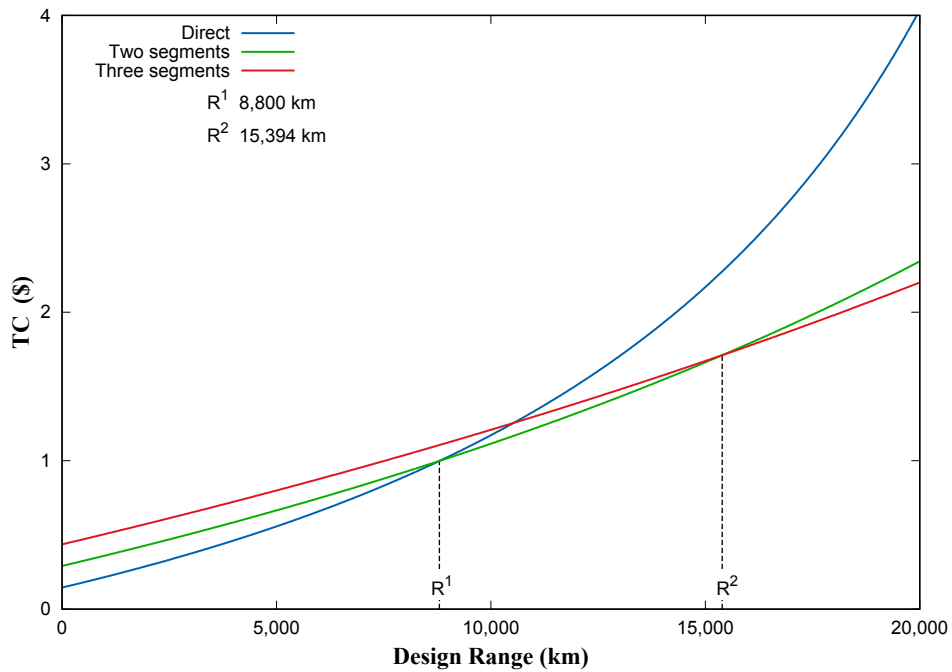


Figure 5: Total Cost against design range: direct flight, two-segment itinerary, and three-segment itinerary; Fixed Cost component of TC is 10 ¢ per payload kg per leg.



## 4 Sensitivity analysis

Green (2002) analyzes the sensitivity of optimal design range to perturbations in the parameters  $c_1$  and  $c_2$ , concluding that  $c_2$  does not affect the optimal design range while the effect of  $c_1$  can be approximated with a quadratic function. In this study we focus on two other key parameters:  $\lambda$  (the lost-fuel fraction of aircraft weight at takeoff) and  $X$  (the aircraft range parameter). Hence the present study is distinct from, but complements that undertaken in Green (2002). We examine the effects of perturbations in  $\lambda$  and  $X$  on optimal design range as well as on the cutoff thresholds that demarcate between optimal one-leg, two-leg, and three-leg segmentation, for both fuel-saving (and hence GHG-saving) and Total-Cost-saving considerations.

Table 2 shows the impact of varying the lost-fuel fraction  $\lambda$ . We continue to use 2.2% as the base value for  $\lambda$ , and we present six scenarios of  $\pm 5\%$ ,  $\pm 10\%$  and  $\pm 20\%$ . For each scenario, the optimal design range and optimal segmentation thresholds are recorded in columns 2–7, together with the associated percentage changes in parentheses. Several conclusions can be drawn from Table 2.

First, an increase in the lost-fuel fraction  $\lambda$  at takeoff leads to longer optimal design range. As more fuel is consumed during takeoff, climb-to-cruise altitude and acceleration-to-cruise speed, the efficiency of short-distance flights drops more sharply than that of longer-distance flights as any increase in  $\lambda$  has a smaller effect due to (averaging over) the higher total mission fuel of longer-distance flights.

Second, as  $\lambda$  increases, the increase in optimal design range leads to higher optimal cutoff thresholds between single-leg and two-leg flights, as well as between two-leg and three-leg flights. When optimal design range is displaced to the right – e.g. as the result of an increase in  $\lambda$  – splitting a journey into separate legs becomes advantageous only at even longer ranges where FPR convexity accelerates the inefficiency penalty accruing from incremental increases in flight distance.

Third, all three variables (columns 2–7) have a closely fitting log-log-linear relationship with  $\lambda$ .<sup>16</sup> For fuel-saving consideration, a 1% change in  $\lambda$  leads to a 0.425% change in optimal design range, a 0.421% change in the two-segment threshold, and a 0.423% change in the three-

---

<sup>16</sup>A log-log-linear relationship in the levels of variables roughly corresponds to a linear relationship in their respective percentage changes.

segment threshold. When minimizing TC instead, a 1% change in  $\lambda$  leads to a 0.100% change in optimal design range, a 0.098% change in the two-segment threshold, and a 0.100% change in the three-segment threshold. Switching from fuel-saving to TC-saving attenuates sensitivity to perturbations in  $\lambda$ . Note that these changes are of the same algebraic sign as the change in  $\lambda$ .

Table 2: Sensitivity of optimal design range and cutoff thresholds to changes in the lost-fuel fraction  $\lambda$ .

Lost-fuel fraction ( $\lambda$ )	Optimal design range (fuel-saving)	Two-segment threshold (fuel-saving)	Three-segment threshold (fuel-saving)	Optimal design range (TC-saving)	Two-segment threshold (TC-saving)	Three-segment threshold (TC-saving)
1.76% (-20%)	3,520 (-9.09%)	4,947 (-8.95%)	8,612 (-8.98%)	6,188 (-2.01%)	8,626 (-1.98%)	15,084 (-2.01%)
1.98% (-10%)	3,702 (-4.39%)	5,196 (-4.36%)	9,047 (-4.39%)	6,253 (-0.98%)	8,712 (-1.00%)	15,235 (-1.03%)
2.09% (-5%)	3,789 (-2.14%)	5,320 (-2.08%)	9,264 (-2.09%)	6,285 (-0.48%)	8,757 (-0.49%)	15,317 (-0.50%)
2.2% (0%)	3,872 (0%)	5,433 (0%)	9,462 (0%)	6,315 (0%)	8,800 (0%)	15,394 (0%)
2.31% (+5%)	3,953 (+2.09%)	5,543 (+2.02%)	9,655 (2.04%)	6,348 (+0.52%)	8,844 (+0.50%)	15,470 (+0.49%)
2.42% (+10%)	4,031 (+4.11%)	5,655 (+4.09%)	9,852 (4.12%)	6,379 (+1.01%)	8,884 (+0.95%)	15,543 (+0.97%)
2.64% (+20%)	4,179 (+7.93%)	5,880 (+8.23%)	10,246 (8.29%)	6,439 (+1.96%)	8,973 (+1.97%)	15,695 (+1.96%)

Table 3 reports the corresponding responses to perturbations of the aircraft range parameter  $X$ . Clearly the optimal design range for single-hop flights as well as the segmentation thresholds are proportional to  $X$ . This is because  $X$  enters the FPR (11) equations – and therefore also the segmentation thresholds (15) and (16) – as the denominator to  $R$ . Therefore when holding optimal range  $R^*$  and all other parameters constant, an arbitrary  $d\%$  ( $d\% \neq 0\%$ ) perturbation of  $X$  renders the original  $R^*$  suboptimal. The first-order condition is restored, however, by scaling  $R^*$  by the same  $d\%$  perturbation. The level of the optimal FPR is left unchanged, although the optimal design range at which this occurs is scaled by  $d\%$  (see column 2). Inspection of equations (15) and (16) confirms that this is true also for the optimal segmentation thresholds (see columns 3–7).

Table 3: Sensitivity of optimal design range and cutoff thresholds to changes in the aircraft range parameter  $X$ .

Range parameter ( $X$ )	Optimal design range (fuel-saving)	Two-segment threshold (fuel-saving)	Three-segment threshold (fuel-saving)	Optimal design range (TC-saving)	Two-segment threshold (TC-saving)	Three-segment threshold (TC-saving)
24,464 (-20%)	3,098 (-20%)	4,346 (-20%)	7,570 (-20%)	5052 (-20%)	7040 (-20%)	12315 (-20%)
27,522 (-10%)	3,485 (-10%)	4,890 (-10%)	8,516 (-10%)	5684 (-10%)	7920 (-10%)	13855 (-10%)
29,051 (-5%)	3,678 (-5%)	5,161 (-5%)	8,989 (-5%)	5999 (-5%)	8360 (-5%)	14624 (-5%)
30,580 (0%)	3,872 (0%)	5,433 (0%)	9,462 (0%)	6315 (0%)	8800 (0%)	15394 (0%)
32,109 (+5%)	4,066 (+5%)	5,710 (+5%)	9,946 (+5%)	6631 (+5%)	9240 (+5%)	16164 (+5%)
33,638 (+10%)	4,259 (+10%)	5,976 (+10%)	10,408 (+10%)	6947 (+10%)	9680 (+10%)	16933 (+10%)
36,696 (+20%)	4,646 (+20%)	6,520 (+20%)	11,354 (+20%)	7578 (+20%)	10560 (+20%)	18473 (+20%)

## 5 Conclusion

In this study we develop a fuel-efficiency model for scheduled passenger air transport built on Küchemann’s (1978) Weight Model and the Breguet Range Equation for cruise fuel consumption. Through a numerical example we show how the model sheds light on the effect of aircraft design range on fuel efficiency. Importantly, it is possible to determine fuel-efficiency-maximizing optimal design range.

Then we introduce a new efficiency metric, the Fuel-Payload Ratio, as an alternative to complement the existing Payload Fuel Efficiency metric. We show that this new metric verifies the conventional representation of the model and furthermore complements the model with new findings. While the PFE curve perfectly captures changing fuel efficiency as a single aircraft is designed for a longer range, FPR gives guidance on how to compare the efficiency levels of multiple aircraft with different design ranges, when aircraft can be grouped to serve a flight route that contains multiple segments. Using the same set of model parameters, we find the cut-off thresholds demarcating between efficiency of a direct flight, an itinerary with two equal segments, and an itinerary with three equal segments.

Moreover, the direct interpretation of FPR as the lower envelope of Total Variable Input curves allows the technical engineering analysis exemplified in Green (2002) to be integrated with the standard cost-curves-based microeconomic efficiency analysis. In this framework we have shown that additional fixed costs on payload have the effect of increasing the cost-efficient design range, causing the latter to diverge from the technically efficient design range. Hence factors that increase payload fixed costs – regardless of where these costs originate from – can have the unintended consequence of contributing to ‘wrong sizing’ of the aircraft stock from the standpoint of fuel efficiency and GHG emissions. Those same factors entail that economically efficient flight-segmentation thresholds occur at much greater origin-destination distances than those which would minimize fuel consumption and GHG emissions.

We study the sensitivity of optimal design range and the cut-off distances for different itinerary structures to model parameters. As the lost fuel fraction  $\lambda$  increases, all the three ranges increase. A 1% change in  $\lambda$  will lead to a 0.421%–0.425% change in the thresholds under pure fuel-saving optimization, and a 0.098%–0.100% change in the thresholds under pure TC-saving optimization. Any change in the aircraft range parameter  $X$ , on the other hand, will

lead to proportionate changes in the thresholds.

## References

- Campbell, S.E, Bragg, M.B., Neogi, N.A., 2013. Fuel-optimal trajectory generation for persistent contrail mitigation. *Journal of Guidance, Control, and Dynamics* 36 (6), 1741–1750.
- Cansino, J.M, Román, R., 2017. Energy efficiency improvements in air traffic: The case of Airbus A320 in Spain. *Energy Policy* 101, 109–122.
- Chi, J., Baek, J., 2012. Price and income elasticities of demand for air transportation: Empirical evidence from US airfreight industry. *Journal of Air Transport Management* 20, 18–19.
- Dallara, E.S., 2011. *Aircraft Design for Reduced Climate Impact*. PhD Dissertation, Stanford University, Stanford, CA.
- Dallara, E.S., Kroo, I.M., 2011. Aircraft design for reduced climate impact. 49<sup>th</sup> AIAA Aerospace Sciences Meeting, 4–7 January 2011, Orlando, FL.
- Dalmau, R, Prats, X., 2015. Fuel and time savings by flying continuous cruise climbs: Estimating the benefit pools for maximum range operations. *Transportation Research Part D* 35, 62–71.
- Dumas, J., Aithnard, F., Soumis, F., 2009. Improving the objective function of the fleet assignment problem. *Transportation Research Part B* 43 (4), 466–475.
- Fielding, J.P., 1999. *Introduction to Aircraft Design*. Cambridge University Press, Cambridge, England.
- Gallet, C.A., Doucouliagos, H., 2014. The income elasticity of air travel: A meta-analysis. *Annals of Tourism Research* 49, 141–155.
- Green, J.E., 2002. Greener by design – the technology challenge. *Aeronautical Journal* 106 (1056), 57–113.
- Green, J.E., 2006. Küchemann’s weight model as applied in the first greener by design technology sub group report: A correction, adaptation and commentary. *Aeronautical Journal* 109 (1099), 361–416.

- Green, J.E., 2009. The potential for reducing the impact of aviation on climate. *Technology Analysis and Strategic Management* 21 (1), 39–59.
- IATA, 2008. Air Travel Demand. International Air Transport Association (IATA) Economics Briefing No. 9, Geneva, Switzerland.
- ICAO, 2012. ICAO Carbon Emissions Calculator, version 5. International Civil Aviation Organization (ICAO), Montréal, Canada. [https://www.icao.int/environmental-protection/CarbonOffset/Documents/Methodology%20ICAO%20Carbon%20Calculator\\_v5-2012\\_Revised.pdf](https://www.icao.int/environmental-protection/CarbonOffset/Documents/Methodology%20ICAO%20Carbon%20Calculator_v5-2012_Revised.pdf)
- Kaivanto, K., Zhang, P., 2017. Rank-order concordance among conflicting emissions estimates for informing flight choice. *Transportation Research Part D* 50, 418–430.
- Küchemann, D., 1978. *The Aerodynamic Design of Aircraft*. Pergamon Press, Oxford.
- Langhans, S., Linke, F., Nolte, P., Gollnick, V., 2013. System analysis for an intermediate stop operations concept on long range routes. *Journal of Aircraft* 50 (1), 29–37.
- Lee, J.J., Lukachko, S.P., Waitz, I.A., Schafer, A., 2001. Historical and future trends in aircraft performance, cost and emissions. *Annual Review of Energy and the Environment* 26, 167–200.
- Li, Z.-C., Lam, W.H.K., Wong, S.C., Fu, X., 2010. Optimal route allocation in a liberalizing airline market. *Transportation Research Part B* 44, 886–902.
- Martinez-Val, R., Perez, E., Cuerno, C., Palacin, J.F., 2013. Cost-range trade-off of intermediate stop operations of long-range transport airplanes. *Proceedings of the Institution of Mechanical Engineers Part G: Journal of Aerospace Engineering* 227 (2), 394–404.
- Nangia, R.K., 2006. Efficiency parameters for modern commercial aircraft, *Aeronautical Journal* 110 (1110), 495–510.
- Perez, R.E., Jansen, P.W., 2014. Design optimization and staging assignment for long-range aircraft operations. In *AVIATION 2014, AIAA/3AF Aircraft Noise and Emissions Reduction Symposium*, 16–20 June 2014, Atlanta Georgia.
- Pita, J.P., Adler, N., Antunes, A.P., 2014. Socially-oriented flight scheduling and fleet assignment model with an application to Norway. *Transportation Research Part B* 61, 17–32.

- Poll, D.I.A., 2011. On the effect of stage length on the efficiency of air transport. *Aeronautical Journal* 115 (1167), 273–283.
- Torenbeek, E., 1997. Cruise performance and range prediction reconsidered, *Progress in Aerospace Sciences* 33 (5/6), 285–321.
- Yutko, B.M., Hansman, R.J., 2011. Approaches to representing aircraft fuel efficiency performance for the purpose of a commercial aircraft certification standard. MIT International Center for Air Transportation, Department of Aeronautics & Astronautics, MIT, Cambridge, MA.
- Zeinali, M., Rutherford, D., 2010. Trends in aircraft efficiency and design parameters. International Council on Clean Transportation, Washington, DC. <http://www.theicct.org/2010/03/trends-aircraft-efficiency/>

## A Mathematical appendix

Noting that the first three derivatives of the FPR function are positive,

$$\text{FPR} = f(R) \quad \text{where} \quad f', f'', f''' > 0 \quad \forall R \in \mathbb{R}_{++} \quad (17)$$

denote the midpoint of the Great-Circle Distance between the origin and the destination airports  $R$  km apart as  $R_0 = R/2$ . Let us conjecture that the minimum whole-itinerary FPR is achieved in a two-leg segmentation when both legs are of length  $R_0$ . With this segmentation, the total FPR is  $2f(R_0)$ . Shortening one leg by  $\Delta \in (0, 0.5]$  entails increasing the length of the other leg by the same amount  $\Delta$  so that total itinerary length remains  $2R_0$ . Now total itinerary FPR may be written as  $f(R_0 - \Delta) + f(R_0 + \Delta)$ . From  $f''' > 0$  it follows that

$$|f(R_0 - \Delta) - f(R_0)| < f(R_0 + \Delta) - f(R_0) \quad (18)$$

and therefore that

$$f(R_0 - \Delta) + f(R_0 + \Delta) > 2f(R_0) \quad \forall \Delta \in (0, 0.5] \quad (19)$$

i.e. that total itinerary FPR is greater under any other division of the total distance than the equal-length-legs segmentation.

Similar reasoning applies in the three-leg case. Redefining  $R_0$  as  $R_0 = R/3$ , let us conjecture that the minimum whole-itinerary FPR in the three-leg segmentation is  $3f(R_0)$ . Define three signed deviation terms  $\Delta_1, \Delta_2, \Delta_3 \in [-0.5, 0.5]$  representing the deviation of legs 1, 2 and 3 from  $R_0$  respectively. These deviation terms satisfy  $\Delta_1 + \Delta_2 + \Delta_3 = 0$ , giving  $(R_0 + \Delta_1) + (R_0 + \Delta_2) + (R_0 + \Delta_3) = 3R_0$ .

If  $\Delta_1, \Delta_2 < 0$  then  $\Delta_3 = |\Delta_1| + |\Delta_2|$ ; if  $\Delta_1, \Delta_3 < 0$  then  $\Delta_2 = |\Delta_1| + |\Delta_3|$ ; if  $\Delta_2, \Delta_3 < 0$  then  $\Delta_1 = |\Delta_2| + |\Delta_3|$ . From  $f''' > 0$  it follows that when  $\Delta_1, \Delta_2 < 0$ ,

$$|f(R_0 + \Delta_1) - f(R_0)| + |f(R_0 + \Delta_2) - f(R_0)| < f(R_0 + |\Delta_1| + |\Delta_2|) - f(R_0) \quad (20)$$

and similarly when  $\Delta_1, \Delta_3 < 0$  and when  $\Delta_2, \Delta_3 < 0$ .

If  $\Delta_1, \Delta_2 > 0$  then  $\Delta_3 = -(\Delta_1 + \Delta_2)$ ; if  $\Delta_1, \Delta_3 > 0$  then  $\Delta_2 = -(\Delta_1 + \Delta_3)$ ; if  $\Delta_2, \Delta_3 > 0$  then  $\Delta_1 = -(\Delta_2 + \Delta_3)$ . From  $f''' > 0$  it follows that when  $\Delta_1, \Delta_2 > 0$ ,

$$(f(R_0 - \Delta_1 - \Delta_2) - f(R_0)) < (f(R_0 + \Delta_1) - f(R_0)) + (f(R_0 + \Delta_2) - f(R_0)) \quad (21)$$

and similarly when  $\Delta_1, \Delta_3 > 0$  and when  $\Delta_2, \Delta_3 > 0$ .

If  $\exists \Delta_i = 0, i \in \{1, 2, 3\}$ , then either there is only one such zero deviation and the problem reduces to that depicted in equations (18) and (19), or then all deviations are zero  $\Delta_i = 0, \forall i \in \{1, 2, 3\}$ .

Therefore

$$f(R_0 + \Delta_1) + f(R_0 + \Delta_2) + f(R_0 + \Delta_3) \geq 3f(R_0) \quad \forall \Delta_i \in [-0.5, 0.5], \quad \sum_{i=1}^3 \Delta_i = 0 \quad (22)$$

i.e. total itinerary FPR is greater under any other division of the total distance than the three equal-length-legs segmentation.

## Highlights

- We derive the Fuel-Payload Ratio (FPR) for parsimoniously segmenting itineraries
- Microeconomic analogue of FPR is Total Variable Input curve with respect to design range
- Economically and technically efficient design ranges diverge due to fixed costs on payload
- Fuel-saving segmentation thresholds respond  $\geq 0.42:1$  to lost-fuel fraction ( $\lambda$ ) %-increases
- Equal-leg-length itineraries are most fuel-efficient

## A Supplementary Appendix: Responses to Reviewers' comments

The authors wish to express their gratitude to the Editor and the Reviewers for these first-round comments, which we find to be valuable and constructive.

In what follows, Reviewers' text is coded **red**. Text cited from the original (first) review draft is coded **blue**. Authors' discussion of Reviewers' comments is coded **black**. Text altered in the body of the article is coded **magenta**.

### Reviewer 1

R1.1 “Authors should make a greater effort explaining why this issue is important. The first paragraph starts with the methods for calculating GHG but the problem has not been contextualized.”

Response: We fully concur with the Reviewer.

Remedy: We have introduced two new lead-in paragraphs, the purpose of which is to provide appropriate contextualization.

New text, p 2: **Air transportation is caught between two converging forcing boundaries. The first is increasing demand for air transportation, driven by income growth – notably, at a rate faster than income growth itself – during an era of consistently increasing world Gross Domestic Product (GDP). [foot-note: In the post-1970s era, GDP has consistently grown, with the exception of one year in which the world economy absorbed the fallout from the financial crisis (2009). The empirical income elasticity of demand for air transportation services is widely documented to be greater than 1: for every 1% increase in income (i.e. GDP), demand for air transport increases by *more* than 1% (IATA, 2008; Chi and Baek, 2012; Gallet and Doucouliagos, 2014).]** The second is accelerating anthropogenic climate change, and the consequent need to reduce greenhouse gas (GHG) emissions drastically in order to avoid global-ecosystem-altering climate change. Technological innovation and far-reaching policy changes will be required in the medium term in order to achieve the targets agreed to in the United Nations Framework Convention on Climate Change (UNFCC COP21).

In the short run, the greenhouse gas (GHG) footprint of air transportation can be reduced by optimizing aircraft design-and-deployment decisions within the envelope of current technological possibility.

- R1.2 “In the introduction section, some acronyms have to be defined the first time is used in the manuscript, i.e. ICAO.”

Response: We thank the Reviewer for detecting these omissions.

Remedy: We have now ensured that all acronyms and initialisms are defined.

- R1.3 “Sections 2, and 3 explain the methodologies that authors have followed in each part of the analysis but they should be linked further previously in the introduction section in order to help readers to understand the complete analysis.”

Remedy: We revise the introduction to provide the reader with a roadmap of how Section 2 lays the theoretical groundwork upon which Section 3 builds to derive the FPR metric and the flight-segmentation results.

Revised text, p 3: In Section 2 we investigate the impact of design range on commercial air transport fuel efficiency by developing a model drawing on Küchemann’s (1978) Weight Model and the Breguet Range Equation for cruise fuel consumption. ... ..We build on this in Section 3 to introduce a new efficiency metric, the Fuel-Payload Ratio (FPR), which captures the technical relationship between mission fuel burn and payload transported to design range. With the aid of this FPR metric, identification of optimal design range (Section 3.2), as well as optimal thresholds for 1-, 2-, and 3-segment flights (Section 3.3), is straightforward. Furthermore,  $1/\text{FPR}$  may be understood as a short-run production function in a standard microeconomic sense, from which it follows that the standard short-run curves – marginal and average product, variable cost and total cost, marginal cost, average variable cost and average total cost – may also be derived straightforwardly. This makes it possible to undertake economic optimization of the design-range decision parsimoniously, without abstracting from any of the engineering information contained in Green’s (2002) PFE metric. We conclude with a sensitivity analysis (Section 4) that complements rather than replicates the sensitivity analysis undertaken

in Green (2002).

- R1.4 “I would suggest to explain further [in] the literature review at the beginning explaining the reason why these three methodologies are applied. Which are the connexions among them?”

Remedy: We follow the Reviewer’s suggestion. The introduction now includes new text that primes the reader to the methodological choices made, and to the connections between the elements of the subsequent analysis.

New text, p 4: ...These two equation families complement each other. Küchemann’s (1978) Weight Model is a standard if not classic [footnote: Dietrich Küchemann is thought by some to be the finest aerodynamicist of his generation. His posthumously published (1978) *The Aerodynamic Design of Aircraft* is widely regarded as a classic text in aerodynamics.] decomposition of aircraft take-off weight into components that roughly correspond to airframe empty weight, payload, engines, and mission fuel. The Breguet Range Equation in turn allows cruise range to be expressed as a function of (i) aircraft initial weight at take-off, (ii) aircraft ‘final weight’ upon landing, after mission fuel has been consumed, and (iii) range-performance parameters capturing the calorific energy content of the fuel, the propulsive efficiency of the engine, and the aircraft design’s lift-to-drag ratio. By substituting terms from one equation into the other and accounting for fuel consumed in propelling the aircraft from the blocks all the way to cruise speed and altitude, Green (2002) derived the Payload Fuel Efficiency (PFE) metric, defined as the product of range and the ratio of the weight of payload to mission fuel. We build on this in Section 3 to introduce a new efficiency metric, the Fuel-Payload Ratio (FPR), which captures the technical relationship between mission fuel burn and payload transported to design range. With the aid of this FPR metric, identification of optimal design range (Section 3.2), as well as optimal thresholds for 1-, 2-, and 3-segment flights (Section 3.3), is straightforward. ...

- R1.5 “In section 4, sensitivity analysis, there is no reference or comparison of the results with other analysis. There is no either an explanation about how difficult is that this might be

implemented.”

Response: Whereas Green’s (2002) sensitivity analysis investigates the effects of perturbations of parameters  $c_1$  and  $c_2$ , the sensitivity analysis conducted in Section 4 of this paper investigates the effects of perturbations of  $\lambda$  (the ‘lost-fuel’ fraction of take-off weight) and  $X$  (the aircraft range parameter). Hence the Section 4 sensitivity analysis *complements* rather than competes with Green’s (2002) sensitivity analysis. A like-for-like comparison with other sensitivity analyses is not possible for this reason.

Remedy: We clarify the complementary nature of the sensitivity analyses conducted in this paper and in Green (2002) in the introduction as well as at the beginning of Section 4.

Revised text, p 4: **We conclude with a sensitivity analysis (Section 4) that complements rather than replicates the sensitivity analysis undertaken in Green (2002).**

Revised text, p 17: **Green (2002) analyzes the sensitivity of optimal design range to perturbations in the parameters  $c_1$  and  $c_2$ , concluding that  $c_2$  does not affect the optimal design range while the effect of  $c_1$  can be approximated with with a quadratic function. In this study we focus on two other key parameters:  $\lambda$  (the lost-fuel fraction of aircraft weight at takeoff) and  $X$  (the aircraft range parameter). Hence the present study is distinct from, but complements that undertaken in Green (2002).**

R1.6 “More efforts should be done by authors to be understood by no specialized readers.”

Response: In addressing the Reviewer’s comments R1.1-5 – as well as in addressing Reviewer #2’s comments R2.1-4 – we have aimed for clarity and simplicity. For instance, we have cut some of the detail on the FPR in the abstract. We have also introduced guidance for the non-specialist in the introduction (see new text above associated with R1.1). In the main body of the text, where simplification would entail glossing over relevant distinctions, we employ structure to aid the reader. For instance as detailed in R1.3, we explain the Breguet Range Equation as consisting of components (i), (ii), (iii). Also, we have added further summary and explanation of our results, such as the following addition to the conclusion:

New text, p 19: Moreover, the direct interpretation of FPR as the lower envelope of Total Variable Input curves allows the technical engineering analysis exemplified in Green (2002) to be integrated with the standard cost-curves-based microeconomic efficiency analysis. In this framework we have shown that additional fixed costs on payload have the effect of increasing the cost-efficient design range, causing the latter to diverge from the technically efficient design range. Hence factors that increase payload fixed costs – regardless of where these costs originate from – can have the unintended consequence of contributing to ‘wrong sizing’ of the aircraft stock from the standpoint of fuel efficiency and GHG emissions. Those same factors entail that economically efficient flight-segmentation thresholds occur at much greater origin-destination distances than those which would minimize fuel consumption and GHG emissions.

## Reviewer 2

R2.1 “... it is not clear the exact contribution with respect to what was already proposed by Green in his previous publications. The new proposed metric is quite similar to already existing metrics and does not seem to provide more insights into the problem assessed. I would like to see a more clear justification of the novelty and contribution of the research done.”

Response: Reflecting upon the Reviewer’s comment, we have come to agree that it is necessary to articulate more clearly this paper’s novel contribution and the way in which it is distinguished from & goes beyond the preceding substantive work by Green (2002, 2006). As it happens, the work program reported here was designed from its very inception to complement Green’s (2002) analysis. Any one study – including Green’s (2002) 57-page-long, broad-ranging paper – must be somehow limited and bounded in its aspirations. Briefly, our paper’s novelty and distinctness occurs in three dimensions.

First, the Fuel-Payload Ratio (FPR) efficiency measure – although derived from the same set of equations Green (2002, 2006) employs – has a direct interpretation in the standard microeconomic framework as the lower envelope of Total Variable Input (TVI) curves, which avails all of the standard microeconomic analysis tools (see Supplementary Figure

6 for illustration).

We now appreciate that this statement in itself is not equally meaningful to all readers, and hence requires elaboration. Responding to this need for elaboration, we introduce an illustration of how Fixed Costs affect Average-Total-Cost-minimizing design range (detailed below in Remedy #2), thereby contributing to our understanding of the empirical disparity between the design ranges of aircraft purchases (and stock thereby created) based on economic drivers and the design ranges of aircraft purchases (and associated stock created) if they were guided purely by technical (fuel, GHG) efficiency.

Second, the present study of flight segmentation aims to sharpen Green's (2002) somewhat vague suggestions concerning stage length, i.e.

...it seems likely that a large aircraft designed to cover long distances in stages of typically, say, 5,000km would have significantly lower seat kilometre costs... (Green 2002, p 61)

...We recommend that a full study be undertaken of the engineering, operational, infrastructure, safety, market, economic and total environmental implications of providing long distance air travel in multi-sector journeys, with no sector longer than, say, 7,500km. (Green 2002, p 61)

...In the full report ... leads to the suggestion that the most environmentally friendly solution might be to break long journeys into sectors not exceeding 7,500km... (Green 2002, footnote, p 61)

Hence the present study is distinct from, but responds to, complements, and sharpens Green (2002).

The advantage of the FPR-based approach is that its mathematical form provides straightforward answers to these types of questions.

Third, the sensitivity analysis reported in this study investigates the effects of variations/perturbations in  $\lambda$  and  $X$  – whereas Green's (2002) sensitivity analysis studies the effects of varying  $c_1$  and  $c_2$ . Hence the present study is distinct from, but complements Green (2002).

Remedy #1: In order to ensure that the paper's findings are more clearly identified and flagged for the reader, separate numbered headings are provided in Section 3.2.

New headings, pp. 8–11:

**Finding 3.1 Mission fuel increases with  $R$ , at an accelerating rate**

**Finding 3.2 min FPR/km design range =  $R^*$**

**Finding 3.3 FPR-based mission fuel is validated by ICAO data**

**Finding 3.4 Standard microeconomic interpretation**

Remedy #2: To illustrate the distinctness of FPR-based analysis and the significance of the standard microeconomic analysis tools that this formulation avails, we illustrate the effect tht a 10¢ increase in Fixed Cost has on economically efficient design range.

New text, pp. 11: **Placing FPR within a microeconomic framework leads to insights that are typically not available within a purely technical engineering analysis. For instance,  $FPR_R = \left(\frac{W_{MF}}{W_P}\right)$  may be re-expressed in monetary-unit terms by multiplying equation (11) by the price of kerosene (\$/kg) – i.e. the vertical axis of Figure 2 may be re-indexed by multiplying by the price of kerosene, which at the time of writing is 654.8 \$/mt or 0.6548 \$/kg (see Figure 3).<sup>17</sup> On this cost scale, the FPR becomes the lower envelope of Total Variable Cost (TVC) curves. This opens up the possibility of investigating the effect of changes in Fixed Costs (FC) on cost-efficient choice of design range – regardless of whether those Fixed Costs arise from engineering, regulatory (e.g. environmental regulations), safety and service, or other business-environment considerations. Figure 3 illustrates how a 10¢ increase in Fixed Cost<sup>18</sup> increases Average-Total-Cost-minimizing design range by over 2,400 km.**

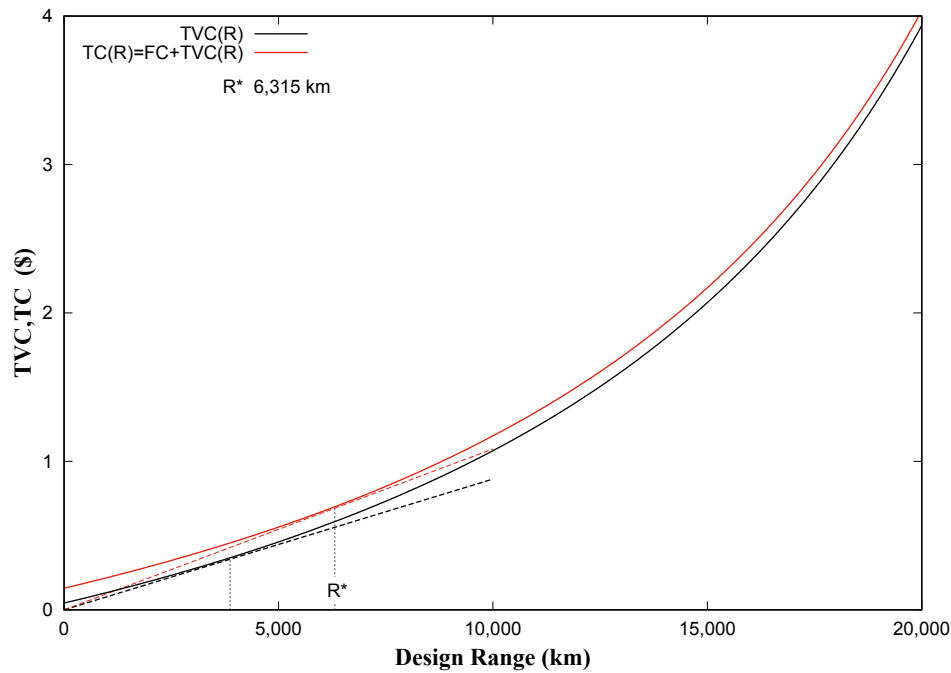
This microeconomic analysis of the effect of Fixed Costs carries two types of implications. First, it goes some way to explaining why the stock of aircraft operated on short- and medium-length segments are ‘oversized’ in terms of design range: economic considerations rather than purely technical fuel- and GHG-efficiency considerations weigh heavily in the aircraft purchase decision. Second, it shows the unintended consequences of introducing regulations – whether motivated by environmental-protection concerns or not – that increase payload Fixed Cost.

---

<sup>17</sup>Jet fuel price obtained from the IATA Jet Fuel Price Monitor on 30 March 2018. <http://www.iata.org/publications/economics/fuel-monitor/Pages/index.aspx>

<sup>18</sup>per kg of payload

**Figure 3: Total Variable Cost (TVC) and Total Cost (TC) envelopes against design range, where Fixed Cost (FC) is 10 ¢ per payload kg.**



Remedy #3: In order to highlight the novelty and precision of the FPR-based approach to determining optimal flight segmentation, we reformat Section 3.3’s introductory-paragraph structure as follows. The mathematical structure presented through equations (15) and (16), and associated proof in Appendix A, are self explanatory.

Reformatted text, p 13 : **Answers to these questions are not straightforward from the PFE-based analysis.**

**The Fuel-Payload Ratio curve, on the other hand, provides straightforward answers to these questions.**

**Since FPR represents the ideal mission-fuel consumption to deliver a one-unit payload to a specified range, when the same unit payload is delivered through segments, the sum of segment-specific FPR ratios represents the total mission fuel for the whole itinerary, assuming that the ideal aircraft (with appropriate design range) is used on each segment. As the FPR curve is convex in design range, this offers unambiguous guidance for minimizing the sum.**

Remedy #4: We revise Section 4’s introductory paragraph to emphasize that the present paper’s sensitivity analysis complements that undertaken in Green (2002).

Original text, p 13: **Green (2002) discusses the sensitivity of optimal design range to the parameters  $c_1$  and  $c_2$ , concluding that  $c_2$  does not affect the optimal design range while the effect of  $c_1$  can be approximated with a quadratic function. In this study we focus on two other key parameters:  $\lambda$  (the lost-fuel fraction of aircraft weight at takeoff) and  $X$  (the aircraft range parameter).**

Revised text, p 17: **Green (2002) analyzes the sensitivity of optimal design range to perturbations in the parameters  $c_1$  and  $c_2$ , concluding that  $c_2$  does not affect the optimal design range while the effect of  $c_1$  can be approximated with with a quadratic function. In this study we focus on two other key parameters:  $\lambda$  (the lost-fuel fraction of aircraft weight at takeoff) and  $X$  (the aircraft range parameter). Hence the present study is distinct from, but complements that undertaken in Green (2002).**

Remedy #5: In the conclusion we include an additional paragraph that summarises some of the further implications of the FPR-based approach.

Revised text, p 19: **Moreover, the direct interpretation of FPR as the lower envelope of Total Variable Input curves allows the technical engineering analysis exemplified in Green (2002) to be integrated with the standard cost-curves-based microeconomic efficiency analysis. In this framework we have shown that additional fixed costs on payload have the effect of increasing the cost-efficient design range, causing the latter to diverge from the technically efficient design range. Hence factors that increase payload fixed costs – regardless of where these costs originate from – can have the unintended consequence of contributing to ‘wrong sizing’ of the aircraft stock from the standpoint of fuel efficiency and GHG emissions. Those same factors entail that economically efficient flight-segmentation thresholds occur at much greater origin-destination distances than those which would minimize fuel consumption and GHG emissions.**

R2.2 “The values given for  $c_1$  and  $c_2$  coefficients seem very arbitrary. Moreover, are they the same for all type of aircraft?”

Response: We agree with the reviewer that inappropriate word choice on our part indeed

conveys the impression that the coefficients are somewhat arbitrarily ‘set’. The sourcing of the values for  $c_1$  and  $c_2$  is detailed at the beginning of Section 2.3. Nevertheless, we very much agree with the Reviewer that this passage requires re-phrasing and elaboration. The parameters capture the way in which fuel (GHG) efficiency changes *across* aircraft of different design range, and are *estimated* from data on 12 different wide-body swept-wing kerosene-fuelled aircraft.

Remedy: We rewrite the paragraph in which the coefficient values are introduced, with the intent of clarifying that these are in actual fact estimated values, rather than values that are arbitrarily ‘set’. And in a footnote, we introduce more detail on how the coefficients have been estimated.

These parameter values are also mentioned at the beginning of Section 3.2 on p 8, as well as in Section 3.3 on p 11. In each case, we rewrite the text, paying careful attention to word choice, and we refer the reader back to Section 3.2 for details.

Original text, p 6: **In order to illustrate how PFE varies with design range, parameter values need to be set for  $X$ ,  $c_1$  and  $c_2$ . Fielding (1999) introduces a method for estimating the values of  $c_1$  and  $c_2$ . Green (2002) adopts 0.3 for  $c_1$  and 2.0 for  $c_2$  for swept-wing kerosene-fuelled aircraft. Green (2006) points out that when reserve fuel is present,  $c_1$  must be adjusted upwards. Following Nangia’s (2006) proposed value of 4.5% of total weight at takeoff as reserve fuel, Green (2006) adjusting  $c_1$  to 0.345. To maintain comparability, we also follow Green (2002) in setting the aircraft range parameter  $X$  to be 30,580km and the lost-fuel fraction  $\lambda$  to be 2.2%.**

Revised text, page 7: **In order to illustrate how PFE varies with design range, parameter values need to be determined for  $X$ ,  $\lambda$ ,  $c_1$  and  $c_2$ . Using Fielding’s (1999) data, Green (2002, 2006) estimates  $c_2$  to be 2.0. Green (2006) revisits the estimation of  $c_1$  in light of Nangia (2006), and using Fielding’s (1999) data Green (2006) estimates  $c_1$  to be 0.345. [footnote: These values for  $c_1$  and  $c_2$  are obtained by fitting  $OEW = (c_1 - 0.045)W_{TO} + (c_2 - 1)W_P$  to Fielding’s (1999) Table A4.5 (page 188) data on twelve modern wide-body, swept-wing, kerosene-fueled passenger aircraft, where the parameter 0.045 reflects Nangia’s (2006) estimate that reserve fuel comprises 4.5% of total weight at takeoff**

(Green, 2006).] We also follow Green (2002, 2006) in employing the aircraft range parameter  $X = 30,580\text{km}$  and the lost-fuel fraction  $\lambda = 2.2\%$ .

Original text, p 8: In this numerical example, we continue to follow Green (2002) in setting 2.0 for  $c_2$  for a swept-wing kerosene-fueled aircraft, and we follow Green (2006) and Nangia (2006) in correcting  $c_1$  upwards from 0.3 to 0.345. Again we follow Green (2002) in setting the aircraft range parameter  $X$  to 30,580km and the lost-fuel fraction  $\lambda$  to 2.2%.

Revised text, page 9: In this numerical example, we continue to employ the parameter values introduced above in Section 2.3. [footnote:  $c_1 = 0.345$ ,  $c_2 = 2.0$ ,  $\lambda = 2.2\%$ ,  $X = 30,580\text{ km}$ ]

Original text, p 11: Using the same numerical assumptions as in previous sections, [footnote: We set 2.0 for  $c_2$  for a swept-wing kerosene-fueled aircraft, and follow Green (2006) and Nangia (2006) in correcting  $c_1$  upwards to 0.345. Again we follow Green (2002) in setting the aircraft range parameter  $X$  to 30,580km and  $\lambda$  to 2.2%.] we plot ...

Revised text, page 14: Using the same numerical estimates as in previous sections [footnote:  $c_1 = 0.345$ ,  $c_2 = 2.0$ ,  $\lambda = 2.2\%$ ,  $X = 30,580\text{ km}$ ] we plot ...

R2.3 “Details on the ICAO data used to assess the FPR curve in figure 2 are missing. At least give a bibliographic reference.”

Response: We thank the Reviewer for spotting this omission.

Remedy: Full reference is provided in a footnote.

Revised text, page 10: Table 1 contains ICAO data on flight range, average mission-fuel consumption and average number of seats (columns 3–5). [footnote: ICAO (2012) documents the methodology by which the average fuel (kg) data have been compiled. The approach employed draws primarily from the EMEP/CORINAIR Emission Inventory Guidebook, following IPCC guidance.]

R2.4 “As a minor suggestion, the authors may consider the following (or similar) two publications to cite in their introduction. These tackle the problem of the flight plan optimisation, which would be a complementary measure to the optimisation of the flight segmentation.”

Response: These are helpful suggestions, and have been integrated into the revisions requested by Reviewer 1 to make the paper more accessible to non-specialized readers, which we have addressed by rewriting parts of the introduction.

Figure 6: Supporting material for Reviewer 2: standard microeconomic analysis tools.

